Acta Pharmaceutica Sinica B 2024;14(6):2613–2630

Chinese Pharmaceutical Association
Institute of Materia Medica, Chinese Academy of Medical Sciences

Acta Pharmaceutica Sinica B

www.elsevier.com/locate/apsb
www.sciencedirect.com

ORIGINAL ARTICLE

Glucagon-like peptide-1 receptor agonists rescued diabetic vascular endothelial damage through suppression of aberrant STING signaling

Xuemin He[a,b,†], Siying Wen[a,b,†], Xixiang Tang[a,b,c,†], Zheyao Wen[a,b], Rui Zhang[a,b], Shasha Li[a,b], Rong Gao[a,b], Jin Wang[a,b], Yanhua Zhu[a,b], Dong Fang[g], Ting Li[a,b], Ruiping Peng[e], Zhaotian Zhang[f], Shiyi Wen[a,b], Li Zhou[a,b,d], Heying Ai[a,b], Yan Lu[d], Shaochong Zhang[g,*], Guojun Shi[a,b,*], Yanming Chen[a,b,*]

[a]*Department of Endocrinology and Metabolic Diseases, the Third Affiliated Hospital of Sun Yat-sen University, Guangzhou 510630, China*
[b]*Guangdong Provincial Key Laboratory of Diabetology & Guangzhou Municipal Key Laboratory of Mechanistic and Translational Obesity Research, the Third Affiliated Hospital of Sun Yat-sen University, Guangzhou 510630, China*
[c]*VIP Medical Service Center, the Third Affiliated Hospital of Sun Yat-sen University, Guangzhou 510630, China*
[d]*Department of Clinical Immunology, the Third Affiliated Hospital of Sun Yat-sen University, Guangzhou 510630, China*
[e]*Department of Ophthalmology, the Third Affiliated Hospital of Sun Yat-sen University, Guangzhou 510630, China*
[f]*State Key Laboratory of Ophthalmology, Zhongshan Ophthalmic Center, Sun Yat-sen University, Guangzhou 510060, China*
[g]*Department of Fundus, Shenzhen Eye Hospital of Jinan University, Shenzhen 518048, China*

Received 8 September 2023; received in revised form 2 January 2024; accepted 2 February 2024

*Corresponding authors.
E-mail addresses: zhangshaochong@gzzoc.com (Shaochong Zhang), shigj6@mail.sysu.edu.cn (Guojun Shi), chyanm@mail.sysu.edu.cn (Yanming Chen).
[†]These authors made equal contributions to this work.
Peer review under the responsibility of Chinese Pharmaceutical Association and Institute of Materia Medica, Chinese Academy of Medical Sciences.

https://doi.org/10.1016/j.apsb.2024.03.011

KEY WORDS

GLP-1 RAs;
STING signaling;
Retinal endothelial cells;
Mitochondrial leakage;
Retinal vascular dysfunction;
Diabetic retinopathy;
CREB;
Inflammation

Abstract Glucagon-like peptide-1 receptor agonists (GLP-1 RAs) protect against diabetic cardiovascular diseases and nephropathy. However, their activity in diabetic retinopathy (DR) remains unclear. Our retrospective cohort study involving 1626 T2DM patients revealed superior efficacy of GLP-1 RAs in controlling DR compared to other glucose-lowering medications, suggesting their advantage in DR treatment. By single-cell RNA-sequencing analysis and immunostaining, we observed a high expression of GLP-1R in retinal endothelial cells, which was down-regulated under diabetic conditions. Treatment of GLP-1 RAs significantly restored the receptor expression, resulting in an improvement in retinal degeneration, vascular tortuosity, avascular vessels, and vascular integrity in diabetic mice. GO and GSEA analyses further implicated enhanced mitochondrial gene translation and mitochondrial functions by GLP-1 RAs. Additionally, the treatment attenuated STING signaling activation in retinal endothelial cells, which is typically activated by leaked mitochondrial DNA. Expression of *STING* mRNA was positively correlated to the levels of angiogenic and inflammatory factors in the endothelial cells of human fibrovascular membranes. Further investigation revealed that the cAMP-responsive element binding protein played a role in the GLP-1R signaling pathway on suppression of STING signaling. This study demonstrates a novel role of GLP-1 RAs in the protection of diabetic retinal vasculature by inhibiting STING-elicited inflammatory signals.

1. Introduction

Diabetic retinopathy (DR) is one of the leading complications of diabetes, with a global prevalence of 22.27%[1]. Intensive control of blood glucose prevents the occurrence and progression of DR, but 30%−50% of diabetic patients still fail to achieve euglycemia[2,3]. The retina is nourished by the choroidal and retinal vascular plexuses, and the latter is further divided into three complexly organized layers: superficial, intermediate, and deep[4]. These retinal vascular plexuses provide large amounts of oxygen and nutrients to maintain visual activities, in which the concentration of neuroglobin is 100-fold higher than that in the brain[5]. Thus, decreased vascular perfusion by constriction of retinal arteries and arterioles results in diabetes-associated ischemia, which then triggers pericyte loss, endothelial cells (ECs) dysfunction, neuron degeneration, immune cell infiltration, and capillary degeneration, leading to vascular leakage and neovascularization[6]. Current therapies mainly target vascular leakage or angiogenesis in the advanced stage of DR, like pan-retinal photocoagulation and intravitreal injection of anti-vascular endothelial growth factor (VEGF), which are invasive and could induce retinal degeneration and fibrosis. It is an urgent need to develop drugs for the prevention and treatment of DR at the early stage, as no therapy has been demonstrated to be effective in the clinic.

Glucagon-like peptide-1 (GLP-1) is highly expressed in the brain, gastrointestinal tracts, and pancreas. However, its physiological function in the retina remains unclear. GLP-1 receptor agonists (GLP-1 RAs) are widely used glucose-lowering drugs, with overt beneficial effects on cardiovascular diseases[7,8]. However, GLP-1 RAs' effects on the microvasculature are controversial, as they showed protective effects on diabetic nephropathy but not on DR[7-11]. In contrast to clinical observations, GLP-1 RAs consistently alleviate DR-related symptoms in laboratory animals[12,13]. GLP-1 RAs activated nitric oxide synthase and promoted the generation of nitric oxide, which increased microvascular perfusion[14,15], although effects on endothelial proliferation and tube formation were not observed[9,16]. It was reported that tissue-specific knockout of GLP-1R in ECs, but not in myeloid cells, abrogated the inhibition of oxidative stress and inflammatory response on the cardiovascular vessels by Liraglutide[17], suggesting that ECs could be a major target of GLP-1 RAs. The roles of GLP-1 RAs in regulating immune cell activation and inflammatory cytokines production have been described in detail[18]; however, the function of GLP-1 RAs on endothelial inflammation and vascular integrity dysregulation in the context of DR remained largely unknown.

The stimulator of interferon genes (STING) signaling pathway was first identified in regulating the innate immune responses. It was later found to play important roles in response to microbial infection and once-immunology as well as tissue damages[19]. Viral DNA and endogenously damaged DNA are sensed and transformed by cyclic GMP-AMP synthase to cyclic dinucleotides. Upon binding with cyclic dinucleotides, STING undergoes conformational changes and forms a protein complex with TANK-binding kinase 1 (TBK1). The complex is then translocated from the endoplasmic reticulum to the Golgi, which subsequently phosphorylates transcriptional factors interferon regulatory factor 3 (IRF3) and nuclear factor kappa B (NF-κB), and activates the transcription of interferons and pro-inflammatory cytokines[20,21]. Recently, increasing studies have revealed a novel role of the STING pathway in vascular and metabolic diseases[22,23]. Deletion or mutation of *Sting* attenuated oxidative stress, inflammation, retinal capillary degeneration, and vascular leakage, protecting against endothelial senescence in diabetic mouse retinas[24]. Our recent study demonstrated that ECs were enriched in *Sting* mRNA expression in the mouse retina, and activation of STING signaling was regulated by the unfolded protein response pathways in ECs[23].

To understand the role of GLP-1 RAs in diabetic vascular damage, the present study evaluated the DR incidence in a retrospective cohort of type 2 diabetic patients taking various medications, and then investigated the retinal damages of *db*/*db* mice after treatment by GLP-1 RAs. By analyzing the RNA sequencing (RNA-seq) data and immunostaining results, we

identified the suppressive effect of GLP-1 RAs signaling on the STING activation, which ameliorated endothelial inflammation and vascular dysfunction both *in vivo* and *in vitro*. Taken together, our results demonstrated the protective effect of GLP-1 RAs on diabetic retinas and the therapeutic potential in treating DR.

2. Materials and methods

2.1. Animal models and treatments

Four-week-old *db*/*db* male mice and age-matched wild-type (WT) male mice were purchased from the Cavens Laboratory Animal Co., Ltd. (China). Mice were maintained *ad libitum*, with free access to food and water under a 12-h light−dark circle, and were randomly divided into groups. Two cohorts of mice received polyethylene glycol Loxenatide (1 mg/kg, Haoseng Pharmaceutical Group Co., Ltd., China) and Semaglutide (0.8227 mg/kg, Novo Nordisk Pharmaceutical Company, Danmol/Lark), respectively (Fig. 3A). For intravitreal injection, mice were anesthetized and pupils were dilated by atropine. Intravitreal injection was performed using the ultrafine micromanipulation pump (World Precision Instruments LLC, USA). Totally 2 μL of saline, Ex-4 (1 mmol/L), or the mixture containing Ex-4 and cyclic AMP response element-binding protein (CREB) inhibitor 666-15 (1 mmol/L for each reagent)[25], were injected into each eye. Intravitreal injection was performed on Day 1 and Day 4, and the experiment was terminated on Day 6. Insulin tolerance test was performed by a single intraperitoneal administration of insulin (Sigma−Aldrich, USA) to WT mice (0.75 U/kg) and *db*/*db* mice (2 U/kg), followed by measurements of blood glucose at 15, 30, 60, and 90 min. Measurement of body composition was conducted by the EchoMRI-500H (EchoMRI™, USA). All the procedures on mice were approved by the Institutional Animal Care and Use Committee of the Third Affiliated Hospital at Sun Yat-sen University (2020000118).

2.2. RNA-seq and single-cell RNA-seq (scRNA-seq) analyses

Retinal samples were sent to the Beijing Genomics Institute for RNA-seq measurement. Analyses were generated based on the FPKM and read counts of target genes. Public raw scRNA-seq datasets of the human eye (GSE201333)[26], fibrovascular membranes (FVM) (GSE165784)[27], and mouse retinas (GSE150703)[28] were downloaded from the Gene Expression Omnibus. The sequencing reads were aligned to the mm10 reference genomes, and unique molecular identifier counts were obtained by Cell Ranger 3.0.2. Cell clusters were annotated according to the reported marker gene expression profiles as described[27]. Individual UMAP plots, violin plots, and correlation plots were generated by the Seurat functions in conjunction with the ggplot2 R packages.

2.3. Fluorescein fundus angiography (FFA)

Anesthetized mice were intraperitoneally injected with 200 μL of 1% sodium fluorescein. Fundus images were captured by the Micron IV funduscopy system (Phoenix Research Labs, USA)[29]. Quantification of vascular tortuosity was performed as described previously[30]. Briefly, images were opened in the Fiji software and changed to 8-bit format. By running the "Trainable Weka Segmentation" in the "Segmentation" menu, a classifier was created to skeletonize the vessels. Vascular tortuosity was calculated by dividing the "Sum of actual branch lengths" by the "Sum of straight lengths between branch nodes (Euclidean distance)".

2.4. Optical coherence tomography (OCT) and electroretinography (ERG)

Mice were anesthetized, and pupils were dilated and kept moist throughout the procedure. Spectral-domain OCT was performed (Bioptigen, Inc., USA)[31]. Total retinal thickness was measured at 1000 μmol/L from the central optic nerve by the ImageJ, and averaged at 3 × 3 grid positions. For ERG measurement, mice underwent dark adaptation for at least 16 h before ERG recording. Serial ERG (RETI PROT/scan21, Roland Consult Electrophysiology and Imaging, Germany) was performed by increasing $cd \cdot s/m^2$. The scotopic flash intensity was set from 0.01, 3.0, and 10 ($cd \cdot s/m^2$), followed by 3.0 $cd \cdot s/m^2$ oscillatory flicker. Then 5-min light adaptation at 10 $cd \cdot s/m^2$ was applied to bleach rods, followed by 3.0 oscillatory potential recording of cone activity. The cone response was measured at 3.0 $cd \cdot s/m^2$ flicker in the presence of rod-desensitizing background white light of 10 $cd \cdot s/m^2$.

2.5. Cell culture and assays

Human retinal vascular endothelial cells (HRVECs) were maintained in DMEM (1 g/L glucose) supplemented with 10% fetal bovine serum and 1% of penicillin and streptomycin. *STING* knockout ($STING^{CRISPR}$) HRVECs were generated using the CRISPR-Cas9 system[23]. Primary brain microvascular endothelial cells (BMECs) were isolated from 4-week-old mice according to an established protocol[32], and maintained in low-glucose DMEM with 20% FBS. Cells were subjected to pre-treatment of 200 nmol/L of exedin-4 (Ex-4) for 24 h, or 666-15 (100 nmol/L) for 2 h, followed by co-treatments of palmitate acid (PA, 200 μmol/L) for 24 h, or high glucose (HG, 30 mmol/L) for 48 h, with bovine serum albumin (BSA) and mannitol as controls, respectively. Treatment of cGAMP (1 ng/mL) was achieved by transfection with lipofectamine 2000 for 24 h, followed by treatment of Ex-4 (200 nmol/L) for another 24 h, with GMP as control. The JC-1 assay kit (Caymen Chemical, USA) was applied to measure the mitochondrial membrane potential according to the manufacturer's instructions. ELISA plate reader was utilized to read out the values of JC-1 aggregates (540 nmol/L) and JC-1 monomers (485 nmol/L). Images were taken immediately and completed within 1 h. Cell viability was also measured by the CCK-8 kit according to the manufacturer's instructions (APExBio, USA).

2.6. Western blot analysis

Retinal samples or cells were lysed in lysis buffer (50 mmol/L Tris-HCl pH 8.0, 1 mmol/L EDTA, 1% TritonX-100, 150 mmol/L NaCl, pH 7.5). Isolation of nuclear fractions was achieved using the Cellular Fragmentation kit (Abcam, USA). Equal amounts of sample lysates were subjected to Western blot analysis. The densitometry of each band was quantified using the Image Lab software (Bio-Rad, USA). Antibodies used in this study are listed in Supporting Information Table S1.

2.7. Quantitative real-time PCR and measurement of mitochondrial DNA (mtDNA)

RNA was extracted using the Takara MiniBEST Universal RNA Extraction Kit, reversely synthesized to cDNA by the Takara

PrimeScript RT-PCR kit, and quantified by the Takara real-time PCR kit. MtDNA was measured by real-time PCR[23]. Briefly, HRVECs were re-suspended in 500 μL extraction buffer and rotated gently for 10 min. After 3 times centrifugation, the supernatants were collected and subjected to the TaKaRa MiniBEST Universal Genomic DNA Extraction Kit for mtDNA extraction. Relative mRNA levels were calculated by ΔC_t values after normalization to GAPDH. Primer sequences were listed as follow: mtDNA forward 5′-CACCCAAGAACAGGGTTTGT-3′, reverse 5′-TGGCCATGGG TATGT TGTTA-3′; *SFXN2* forward 5′-GCTCCAGTTCTACAGG ACGATG, reverse 5′-GTGGCTGTGAAGTAGGAAAGGG-3′; *SLC8B1* forward 5′-ATGGTGGCTGTGTTCCTGACCT-3′, reverse 5′-GGTGCAGAGAATCACAGTGACC-3′.

2.8. Immunostaining

The FVM was collected from the necessary surgeries required for treatment of proliferative DR, and immediately fixed in 4% paraformaldehyde. Eyeballs of mice were gently removed and fixed in 4% paraformaldehyde for 10 min, and transferred to 2× PBS for 10 min. Then the retinas were isolated, mounted, and stored in 100% methanol at −30 °C. Paraffin-embedded retinal sections underwent serial steps of dewax and rehydration, and antigen was retrieved in boiling citrate buffer (10 mmol/L sodium citrate, 0.05% Tween 20, pH 6.0). Cells were washed by ice-cold PBS 3 times, and fixed in 4% paraformaldehyde for 15 min. For VE-cadherin staining, HRVECs must be seeded in a collagen-coated chamber, and maintained at 100% confluence for at least 2 days before staining. Blocking and penetration were performed by incubation in 5% BSA with 0.3% Triton at room temperature for 1 h. Primary antibodies were incubated at 4 °C overnight, followed by secondary antibodies at room temperature for 2 h. An anti-fade mounting medium (VectorShield, USA) was applied, and images were captured under a confocal microscope. Analysis of vasculature and immunostaining was performed by the AngioTool[33] and Fiji software.

2.9. Study population

Information of 34,011 diabetic inpatients, who were admitted to the Third Affiliated Hospital of Sun Yat-sen University from January 2011 to January 2020, was collected from the Diabetes Medical Database of the Department of Endocrinology and Metabolic Diseases[34]. First of all, 836 cases of non-type 2 diabetes and 20,241 cases without 2 medical records were excluded; then 8908 patients with pre-existed microvascular complications (MVC) and 3027 patients with less than 1-year follow-up were excluded; moreover, 28 cases combined usage of drugs and 1348 cases without testing laboratory results were excluded; finally, 1626 type 2 diabetic patients without MVC at admission were included for analysis. Patients were followed until diagnosis of DR or until the end of this study (31st January 2020). Clinical and laboratory data from the first and last visits, including demographic characteristics, laboratory tests, and medication usage, were collected. Type 2 diabetes was diagnosed according to the 1999 Guidelines of the World Health Organization. Fundus images were utilized for the diagnosis of DR based on the International Clinical Classification Criteria for Diabetic Retinopathy. This study was approved by the Ethics Committee of the Third Affiliated Hospital of Sun Yat-sen University, registered at https://clinicaltrials.gov/ (NCT02 587741), and performed according to the principles of the Declaration of Helsinki. The FVM was collected from the necessary surgeries required for the treatment of proliferative DR from seven patients. Written consent was obtained from proliferative DR patients before surgery.

2.10. Statistical analyses

Statistical analysis of the retrospective cohort study was performed using SPSS 22.0 for Windows (SPPS Inc., USA). Descriptive statistics are expressed as mean ± standard deviation (SD) or median (25th; 75th percentiles) for continuous variables or numbers for categorical variables in the cohort study. Differences in continuous variables between groups were evaluated by Student's *t*-test, while differences in categorical variables between groups were analyzed by the χ^2 test. The relationships between GLP-1 RAs and the incidence of DR were estimated by calculating odds ratios and 95% confidence intervals using logistic regression. Then, three multivariate logistic regression models were performed to adjust for confounding factors. Model 1 was adjusted for age and sex. Model 2 was additionally adjusted for HbA1c. Model 3 was additionally adjusted for body weight, triglyceride, LDL-C, HDL-C, creatinine, and insulin usage. Subgroup analyses were performed based on age (<50 and >50 years) and HbA1c levels (<7.0% and >7.0%). Analysis of covariance was used to compare the change in body weight, HbA1c, triglyceride, LDL-C, and HDL-C after treatment. Animal and cellular results are expressed as the mean ± standard error of the mean (SEM). Comparisons were performed with unpaired and paired *t*-tests. When multiple comparisons were performed, one-way ANOVA was used. A 2-tailed $P < 0.05$ was considered as statistical significance.

3. Results

3.1. Decreased DR incidence by GLP-1 RAs and detection of GLP-1R in the FVM in type 2 diabetic patients

Previous clinical studies showed controversial outcomes of GLP-1 RAs in patients with DR[35]. However, these results were not conclusive due to various limitations, such as DR was not set as the primary outcome, or the baselines of DR were unclear. Thus, we conducted a retrospective cohort study with the primary outcome being DR-related symptoms. The medical records of 34,011 inpatients at the Third Affiliated Hospital of Sun Yat-sen University from 2011 to 2020 were collected. After serial steps of exclusions, 1626 type 2 diabetic patients without MVC were admitted for analysis (Fig. 1A). According to the medication history, these patients were divided into 3 groups: 99 patients in the GLP-1 RAs group, 1045 patients in the oral antidiabetic drugs (OAD) group, and 482 patients in the insulin group (Fig. 1B). Basal demographics and clinical characteristics of patients were listed in Supporting Information Table S2. The median follow-up time was 2.8 years (Fig. 1C). Compared to the insulin and OAD groups, the GLP-1 RAs group showed significantly decreased DR incidence (Fig. 1D, Table 1), accompanied by reduced body weight and HbA1c (Fig. 1E and F), unchanged LDL-C and HDL-C levels, and slightly increased triglyceride levels (Fig. 1G–I). In univariate logistic regression analysis (Table 2), the use of GLP-1 RAs was associated with a lower incidence of DR (OR = 0.293, 95% CI: 0.092, 0.937, $P = 0.039$). After adjusting for age and gender, the multivariate logistic regression analysis (Model 1) showed that the use of GLP-1 RAs was still significantly correlated to a lower incidence of DR. When

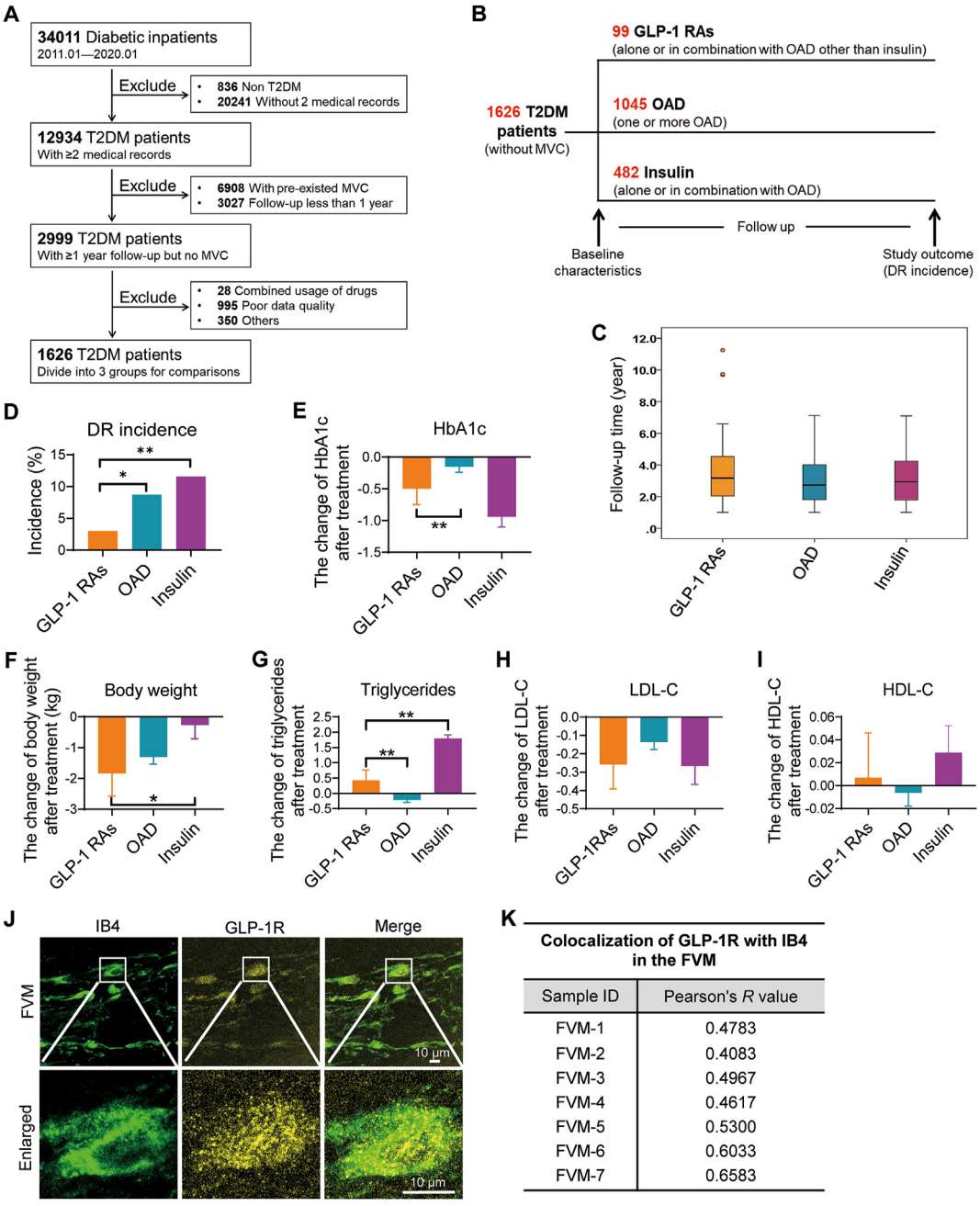

Figure 1 Decreased DR incidence in type 2 diabetic patients with GLP-1 RAs utilization and measurement of GLP-1R in the FVM. (A) Flow chart of the exclusion steps in the retrospective cohort study. (B) Illustration of the grouping strategy based on the medication history. (C) Follow-up time, (D) DR incidence, and levels of HbA1c (E), body weight (F), triglycerides (G), LDL-C (H), and HDL-C (I) in these three groups. (J, K) Immunostaining of GLP-1R (yellow) together with IB4 (green), and percentage of $IB4^{+}GLP\text{-}1R^{+}$ cells in the FVM from type 2 diabetic patients with proliferative DR ($n = 7$, scale bar = 10 μm). Data are expressed as mean ± SEM; $^{*}P < 0.05$, $^{**}P < 0.01$.

Table 1 Relative risk (RR) for the association between the usages of GLP-1 RAs compared with the uses of OAD or insulin treatment and the risk of DR.

Exposure	Event	Incidence risk	RR	95%CI
OAD	91	8.7%	1	reference
GLP-1 RAs	3	3.0%	0.349	0.113−1.080
Insulin treatment	56	11.6%	1	reference
GLP-1 RAs	3	3.0%	0.276	0.090−0.845

Table 2 Regression analysis of the relationship between the incidence of DR and GLP-1 RAs users.

Treatment	Univariate		Model 1		Model 2		Model 3	
	OR (95% CI)	*P*-value	OR (95% CI)	*P*-value	OR (95% CI)	*P*-value	OR (95% CI)	*P*-value
GLP-1 RAs	0.293 (0.092, 0.937)	0.039	0.222 (0.064, 0.771)	0.018	0.293 (0.070, 0.884)	0.031	0.442 (0.116, 1.681)	0.231
Stratified by age								
≤50 year	0.415 (0.055, 3.131)	0.393	0.350 (0.044, 2.769)	0.320	0.289 (0.036, 2.303)	0.241	0.298 (0.032, 2.788)	0.288
>50 year	0.340 (0.081, 1.424)	0.140	0.058 (0.011, 0.294)	0.001	0.056 (0.010, 0.326)	0.001	0.164 (0.024, 1.137)	0.067
By HbA1c levels								
≤7.0%	0.000 (0.000, −)	0.998	0.000 (0.000, −)	0.998	0.000 (0.000, −)	0.998	0.000 (0.000, −)	0.998
>7.0%	0.301 (0.094, 0.970)	0.044	0.233 (0.067, 0.812)	0.022	0.306 (0.088, 1.073)	0.064	0.467 (0.124, 1.752)	0.259

Model 1: Adjusted for age, gender.
Model 2: Adjusted for age, gender, HbA1c.
Model 3: Adjusted for age, gender, weight, HbA1c, TG, HDL-C, LDL-C, Cr, insulin user.

additionally adjusting for HbA1c, the use of GLP-1 RAs remained independently associated with the lower incidence of DR (Model 2). Further subgrouping of patients based on HbA1c or age showed that patients with poor control of blood glucose (HbA1c>7%), or age>50 years, experienced reduced incidence of DR with GLP-1 RAs treatment (Model 1). However, no significant correlation was identified between the use of GLP-1 RAs and DR incidence by multivariate regression analysis (Model 3).

The expression of GLP-1R was a critical indicator of the effectiveness of GLP-1 RAs. To understand whether proliferative DR was responsive to GLP-1 RA treatment, we performed immunostaining and detected relatively high levels of GLP-1R in the FVM, which co-localized with isolectin B4 (IB4) that ranged from 40% to 66% (Fig. 1J and K). Taken together, treatment by GLP-1 RAs is associated with decreased DR incidence, and might be effective in attenuating DR in type 2 diabetic patients due to the relatively high levels of GLP-1R in the FVM.

3.2. Down-regulation of GLP-1R in the retinal vessels of diabetic mice

Previous reports on GLP-1R distribution in the retina were inconsistent due to the limitations of antibodies[13,36]. To circumvent this problem, we analyzed the public scRNA-seq data from the human retina. As shown in Fig. 2A, the expression of *GLP-1R* mRNA was low, and only detected in vascular ECs, dendritic cells, and T cells in the human retina. Then we confirmed the *GLP-1R* mRNA expression in a retinal vascular endothelial cell line HRVECs, which was detectable and down-regulated by PA treatment (Fig. 2B). We further compared the expression levels of GLP-1R in the retinas from WT and *db/db* mice. Blood glucose levels of *db/db* mice suggested hyperglycemia, which is essential for DR development (Fig. 2C). As shown in Fig. 2F, the retinal vasculature is composed of three layers: superficial, intermediate, and deep. Immunostaining of retinal sections and flatmounts revealed a significant reduction of GLP-1R protein levels in the retinas of *db/db* mice compared to controls (Fig. 2D, E, G, H), which was consistent with the observation in the retina of diabetic patients[13]. Notably, GLP-1R protein was enriched in the three retinal vascular layers (Fig. 2G), further supporting the data of the human retina by scRNA-seq (Fig. 2A). These data indicate that GLP-1R is expressed in retinal endothelial cells, and is decreased by diabetes.

3.3. Improved visual activities and reduced retinal cell death by GLP-1 RAs treatment through suppression of inflammation in diabetic retinas

To test the effect of GLP-1 RAs on DR, semaglutide and lixenatide were administrated to two different cohorts of mice for 10 weeks (Fig. 3A). For convenience in the following statements, WTS and WTG stood for WT mice receiving saline and GLP-1 RAs, respectively; DBS and DBG stood for *db/db* mice receiving saline and GLP-1 RAs, respectively. Compared to DBS mice, DBG mice showed a significant reduction in random and fasting blood glucose levels, but an increase in body weight (Supporting Information Fig. S1A−S1D). Moreover, insulin sensitivity was improved by GLP-1 RAs treatment in both WT mice and *db/db* mice (Fig. S1E and S1F).

As declined neuronal activities were accompanied by vascular dysfunctions, we measured the neuronal functions of the retina by ERG. As illustrated in Fig. 3B, the amplitude of scotopic a wave and b wave are increased with the intensities of flashes. Both

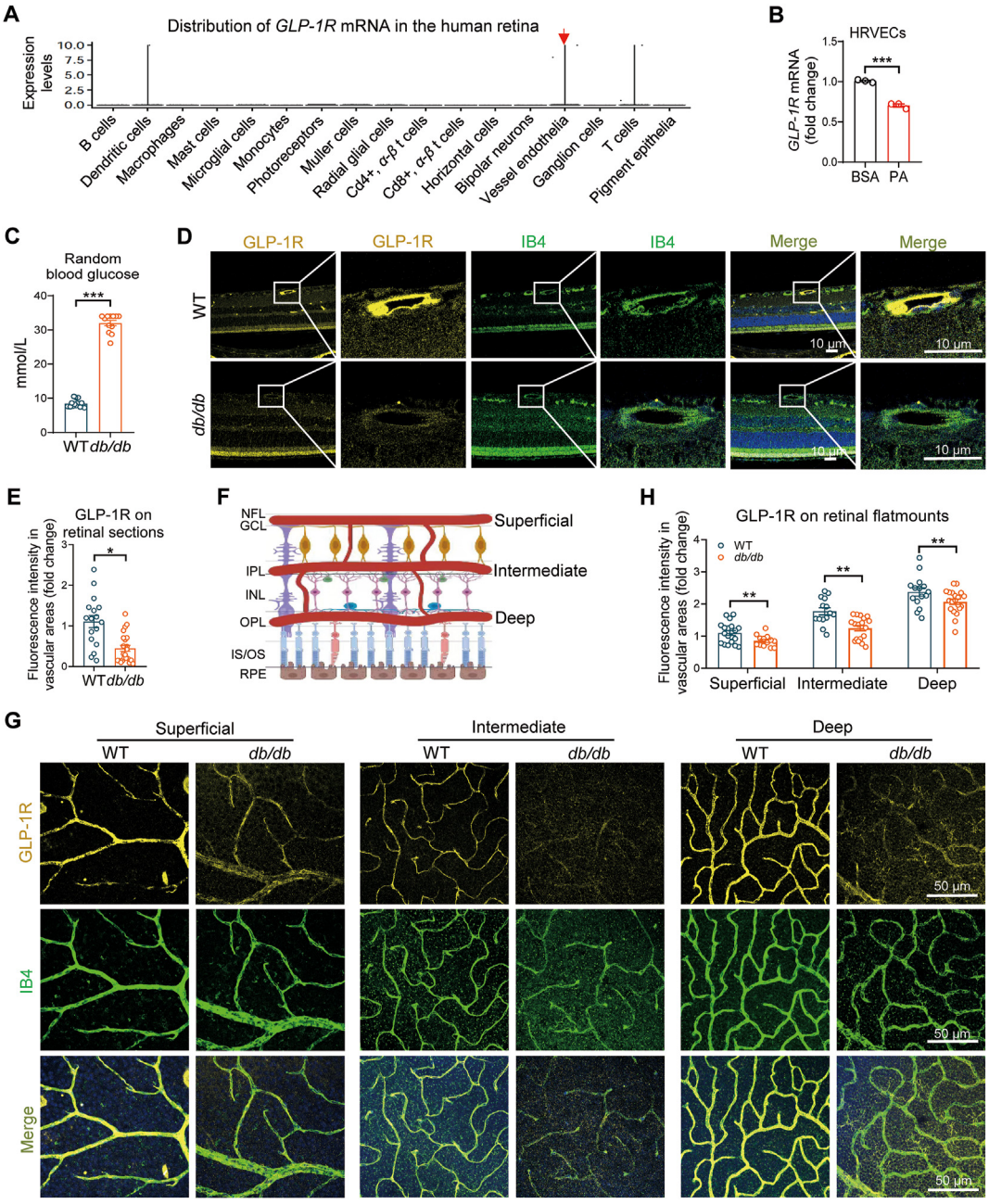

Figure 2 The levels of GLP-1R were decreased in the mouse retinal vessels with DR. (A) Distribution of *GLP-1R* mRNA in the human retina revealed by scRNA-seq analysis. (B) Real-time PCR measurement of *GLP-1R* mRNA levels in HRVECs after treatment of PA (200 μmol/L) or the same volume of BSA for 24 h ($n = 3$). (C) Random blood glucose levels of 18-week-old *db/db* mice and WT mice ($n = 9–13$). (D, E, G, H) Immunostaining of GLP-1R (yellow) together with IB4 (green), and quantification of fluorescence intensity in retinal paraffin sections ($n = 5$, scale bar = 10 μm) and retinal flatmounts ($n = 5$, scale bar = 50 μm) from 18-week-old *db/db* mice and WT mice. (F) Illustration of the three vascular plexuses in the retina. Data are expressed as mean ± SEM; $^{*}P < 0.05$, $^{**}P < 0.01$, $^{***}P < 0.001$.

scotopic a wave and b wave were significantly increased in the DBG group relative to DBS controls (Fig. 3C and D), indicating improvements in photoreceptor and bipolar functions. Moreover, retinas from DBG mice displayed increased scotopic oscillatory potential (Fig. 3E and F), which suggested better retinal adaptive response, and augmented photopic flicker amplitude, implicating less retinal vein occlusion by GLP-1 RA treatment. These observations were consistent with a previous study that GLP-1 RA eye drops enhanced neuronal functions of the retina in diabetic mice[12].

As neuronal dysfunction could be triggered by inflammation, we tested glial fibrillary acidic protein (GFAP), a marker of activated Müller glia and astrocytes. Indeed, diabetes increased the number of GFAP-positive cells, which was reversed by GLP-1 RA treatment (Fig. 3G and H). Consistently, gene set enrichment analysis (GSEA) analysis of the transcriptomic data of these retinas revealed improved neuronal activities and reduced inflammatory response by GLP-1 RA treatment (Fig. 3I). In addition, we examined the retinal thickness by OCT, which is an indicator of retinal degeneration[37], and demonstrated that the retinas of DBS mice were thinner compared with those

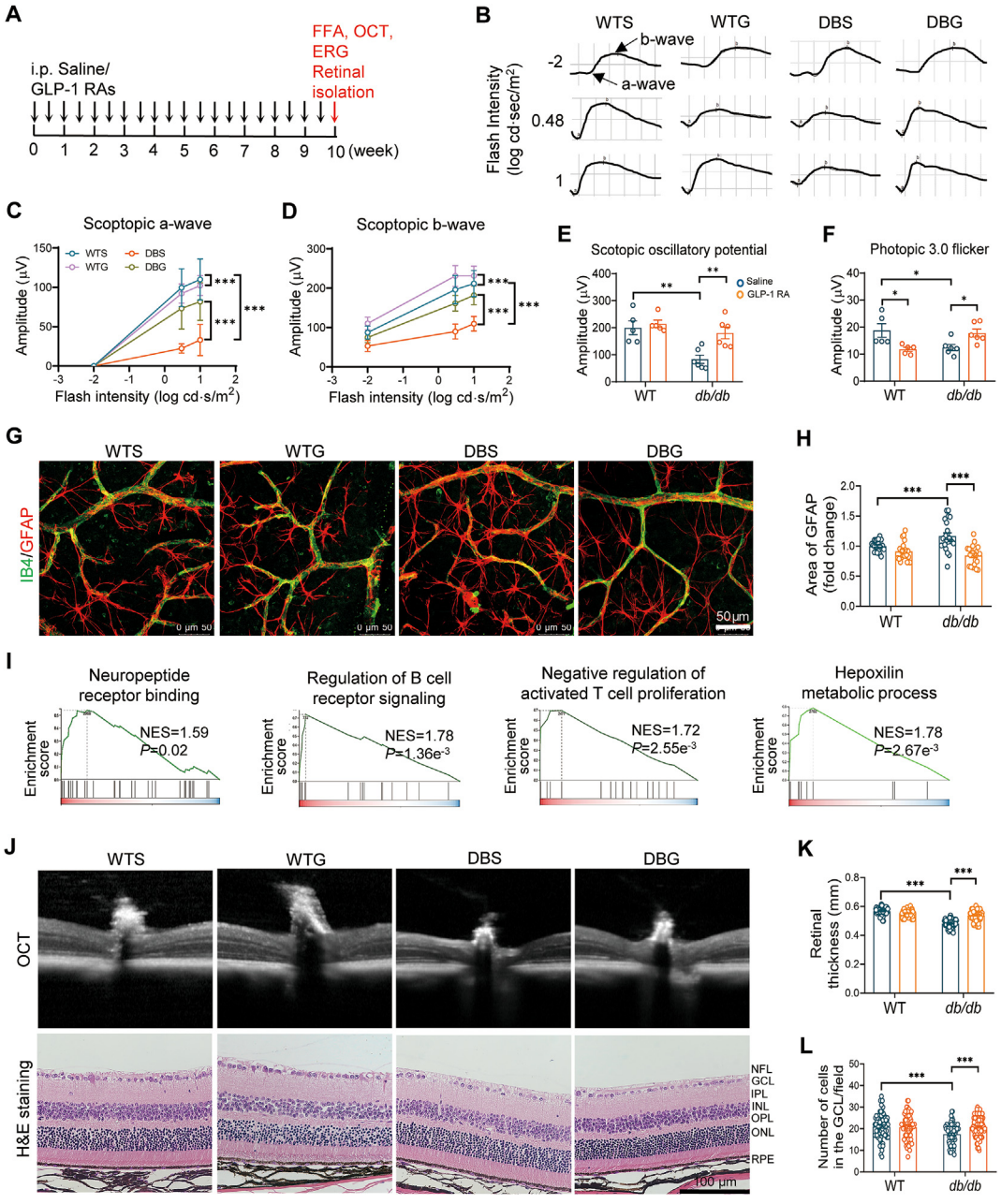

Figure 3 GLP-1 RAs improved retinal neuronal activities and suppressed inflammation in *db*/*db* mice. (A) Timeline of GLP-1 RAs treatments and measurements in the mice. (B) Illustration of the ERG curves of a-wave and b-wave. (C−F) Quantification of (C) scotopic a-wave, (D) scotopic b-wave, (E) scotopic oscillatory potentials, and (F) photopic 3.0 flicker in the retinas of 18-week-old *db*/*db* mice and WT mice (n = 9−13). (G, H) Immunostaining and quantification of GFAP (astrocyte marker, red) and IB4 (green) in the superficial layer of retinal flatmounts (n = 3, scale bar = 50 μm). (I) GSEA analysis of neuronal activity and inflammatory pathways in the DBG retinas compared to the DBS controls. (J−L) OCT and quantification of central retinal thickness (n = 5), as well as H&E staining, and quantification of cell numbers in the ganglion cell layer of *db*/*db* mice and WT mice (n = 5−6, scale bar = 100 μm). ERG, OCT, and staining of GFAP were performed on the mice using Semaglutide; RNA-seq analyses and H&E staining were performed on the mice using Loxenatide. Data are expressed as mean ± SEM; *P < 0.05, **P < 0.01, ***P < 0.001.

of WT controls, whereas GLP-1 RA treatment increased the thickness of retinas (Fig. 3J and K). Cell death in the ganglion cell layer was also reduced in DBG retinas compared to DBS controls as shown by H&E staining (Fig. 3J and L). These data indicate that GLP-1 RAs treatment improves visual activities and reduces retinal cell death by suppressing inflammation in diabetic retinas.

3.4. Reduced acellular capillaries and preserved vascular integrity in diabetic retinas after GLP-1 RAs treatment

As GLP-1R was highly expressed in retinal vessels, we hypothesized that retinal vessels were a major target of GLP-1 RAs. Treatment of GLP-1 RA significantly reduced vascular

tortuosity in *db*/*db* mice evaluated by FFA assays (Fig. 4A and B), which was increased by diabetes[38]. To understand the molecular mechanisms of GLP-1 RAs in the retina, the heat map and principal component analysis were generated and demonstrated that DBG retinas displayed different expression profiles from DBS controls (Supporting Information Fig. S2A−S2D). In particular, the components of the inner blood-retina barrier (BRB), such as extracellular matrix (ECM) genes *Cldn5*, *Cd34*, *Col4a3*, and *Col23a1*, were significantly altered by GLP-1 RA treatment (Fig. 4C). GSEA of the gene ontology pathways

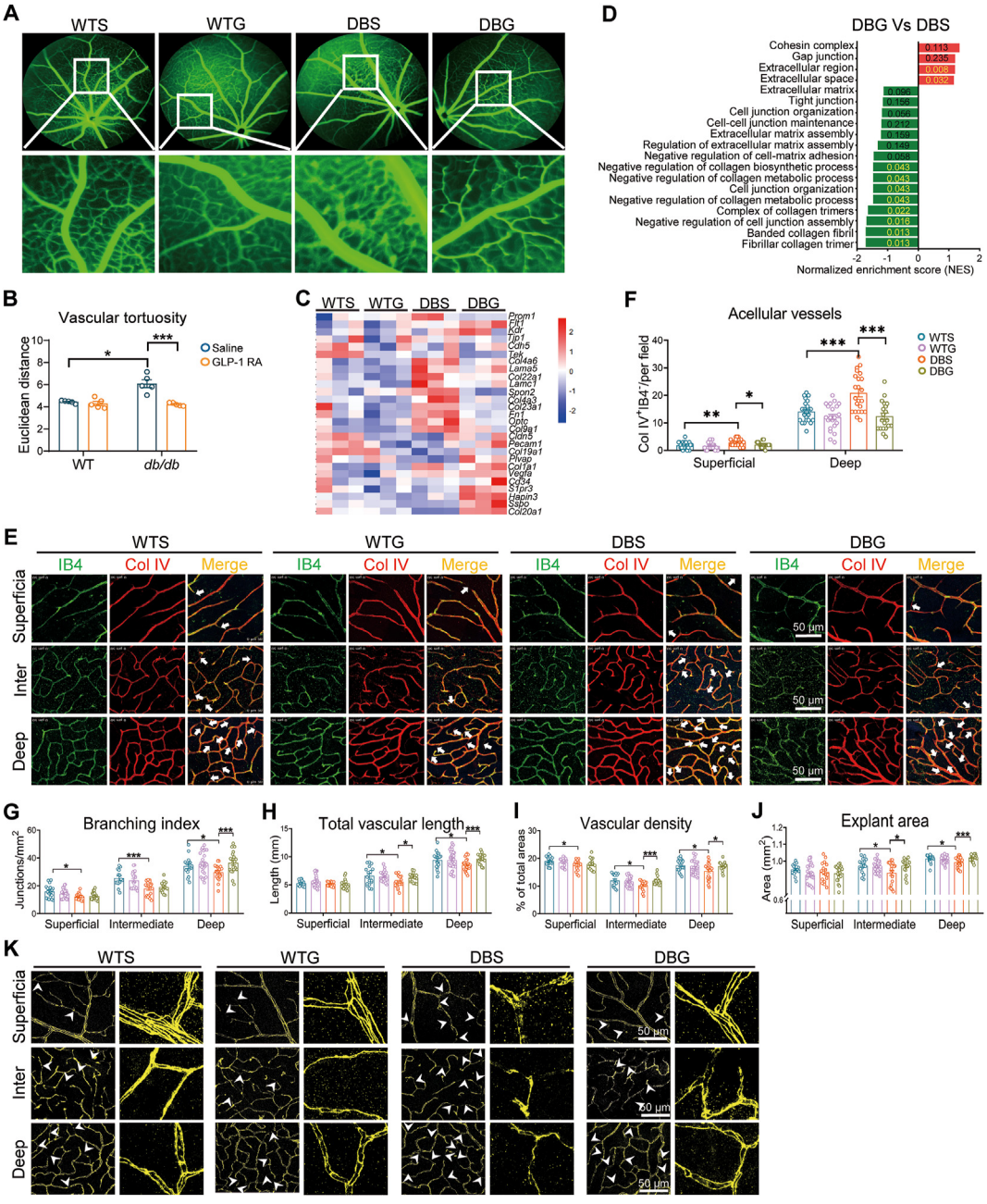

Figure 4 GLP-1 RAs preserved the integrity and functions of the retinal vessels of *db*/*db* mice. (A, B) FFA and quantification of retinal vascular tortuosity in 18-week-old *db*/*db* mice and WT mice ($n = 5$). (C) Heat map of ECM components, junctional proteins, endothelial markers, and angiogenic factors, and (D) GSEA analysis of junctional and ECM signaling pathways in the retinas ($n = 3$). (E−J) Co-staining of IB4 (green) and collagen IV (red), and quantification of acellular vessels, branching index, total vascular length, vascular density, and explant area in the superficial, intermediate, and deep layer of the retinal vasculature ($n = 3$−5, scale bar = 50 μm). (K) Staining of claudin-5 in retinal samples. White arrows indicated broken lines of claudin-5 at the junctional site of the vasculature ($n = 3$, scale bar = 50 μm). FFA and staining of collagen IV were performed on the mice using semaglutide; RNA-seq analyses and staining of claudin-5 were performed on the mice using loxenatide. Data are expressed as mean ± SEM; $^{*}P < 0.05$, $^{**}P < 0.01$, $^{***}P < 0.001$.

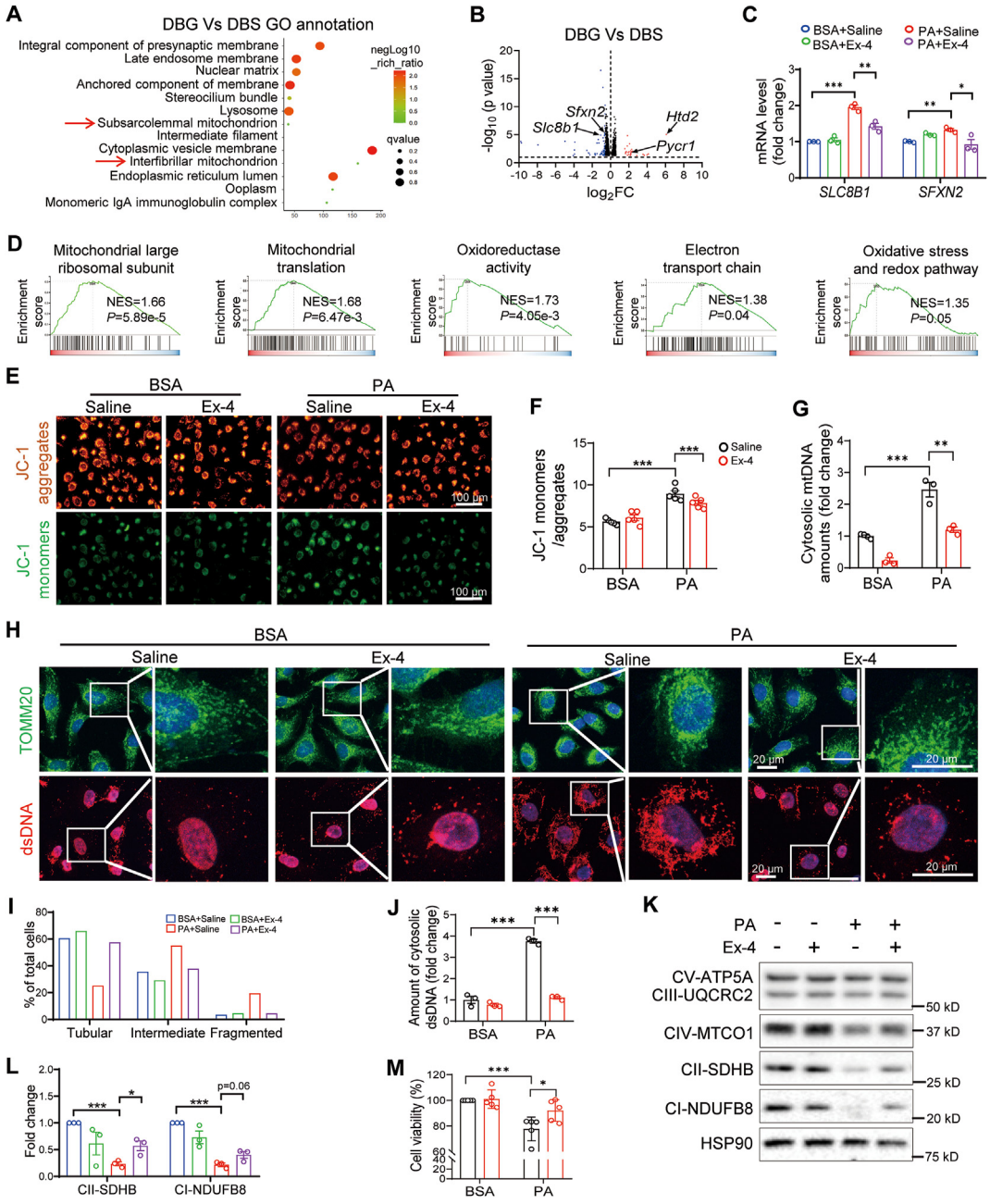

Figure 5 GLP-1 RAs preserved the mitochondrial integrity and maintained the redox balance in retinal ECs. (A) GO analysis of the topmost changed cellular components, (B) volcano plot of 18,439 genes, and (D) GSEA of mitochondria-related pathways in the DBG retinas relative to DBS controls. Genes with fold change <0.66 or ≥1.5, and $P < 0.05$ were considered significantly changed. Down-regulated genes were represented by blue dots and up-regulated genes by red dots. Arrows indicated significantly changed mitochondria-related molecules ($n = 3$). (C) Real-time PCR measurement of *SLC8B1* and *SFXN2* ($n = 3$), (E, F) Immunostaining and quantification of JC-1 monomers and aggregates ($n = 6$, scale bar = 100 μm), (G) real-time PCR measurement of mtDNA amounts ($n = 3$), (H) immunostaining of TOMM20 (green, scale bar = 20 μm) and dsDNA (red, scale bar = 20 μm), (I) quantification of the percentage of tubular, intermediate and fragmented mitochondria, (J) quantification of cytosolic dsDNA amounts ($n = 6$), (K) Western blot analysis of five OXPHOS proteins including CV-ATP5A, CIII-UQCRC2, CIV-MTCO1, CII-SDHB, and CI-NDUFB8, (L) densitometry quantification of CII-SDHB and CI-NDUFB8, and (M) cell viability measured by the CCK-8 kit in HRVECs pre-treated by Ex-4 (200 nmol/L) for 24 h, followed by treatment of PA (200 μmol/L) or BSA for 24 h ($n = 3$). RNA-seq analyses were performed on the mice using loxenatide. Data are expressed as mean ± SEM; $^{*}P < 0.05$, $^{**}P < 0.01$, $^{***}P < 0.001$.

further demonstrated significant increases in ECM space and region, and suppression on the negative regulation of collagen-related and junctional pathways (Fig. 4D).

Co-staining of collagen IV and IB4 indicated fewer avascular capillaries in DBG retinas compared to DBS controls (Fig. 4E and F), which indicates less endothelial cell death in diabetic retinas[24]. In addition, the vascular density, total vascular length, branching index, and explant areas were also improved by GLP-1 RA treatment (Fig. 4G−J). Breakdown of the inner BRB is an overt symptom of DR. Claudin-5 is the most abundant among claudin proteins in the inner BRB[39], which is down-regulated and re-oriented under diabetes, leading to vascular permeability[40]. As shown in Fig. 4K, DBS retinas exhibited more areas lacking claudin-5 at the endothelial junctions, while DBG retinas displayed a better-organized orientation and elongation pattern of claudin-5. Taken together, these data indicate that GLP-1 RA treatment protects against damage to the vascular morphology and integrity in diabetic retinas.

3.5. *Preservation of the mitochondrial integrity and maintenance of the redox balance by GLP-1 RAs treatment in retinal ECs*

It has been reported that astrocyte-specific deletion of GLP-1R impaired the integrity and respiration capacity of the mitochondria in the astrocytes, which are essential for the functionality of the inner BRB[41]. Consistently, gene ontology analysis of the retinal transcriptomic data suggested that the expression levels of mitochondrial genes were dramatically altered by GLP-1 RA treatment in *db*/*db* mice (Fig. 5A). Volcano plot analysis further identified several mitochondrial genes that were significantly changed in the retinas of DBG mice compared with those of DBS mice (Fig. 5B). For example, the mRNA levels of sideroflexin 2 (*Sfxn2*), which accommodates mitochondrial iron metabolism, and solute carrier family 8 member B1 (*Slc8b1*), which encodes sodium/calcium transports to control the calcium efflux in the mitochondria, were significantly reduced by GLP-1 RA treatment. Besides, the expression of hydroxyacyl-thioester dehydratase type 2 (*Htd2*), a gene that regulates fatty acid metabolism, and pyrroline-5-carboxylate reductase 1 (*Pycr1*), a gene that generates $NADP^+$, were significantly induced by GLP-1 RA treatment. The altered gene expression patterns were also confirmed in HRVECs by real-time PCR. As shown in Fig. 5C, Ex-4 treatment suppressed the PA-induced expression of *SLC8B1* and *SFXN2*. The GSEA analysis also revealed that mitochondrial protein translation and the redox balance were improved by GLP-1 RA treatment (Fig. 5D).

The JC-1 is a dye to visualize the energetic status of the mitochondria in alive cells. When the mitochondrial membrane potential is decreased (unhealthy status) or the mitochondrial number is low, less JC-1 is allowed into the mitochondria and exists as monomers. *Vice versa* and exists as aggregates. Thus, a higher ratio of JC-1 aggregates to monomers indicates healthier mitochondria and is more potent in generating ATP[42]. PA treatment significantly induced the JC-1 monomers to aggregates ratio in HRVECs, suggesting a reduced capacity in generating ATP in the mitochondria; interestingly, Ex-4 treatment potently reversed PA-induced mitochondrial defects (Fig. 5E and F). Likewise, Ex-4 counteracted mtDNA leakage into the cytosol induced by PA treatment (Fig. 5G). Immunostaining of translocase of outer mitochondrial membrane 20 (TOMM20) and double-strand DNA (dsDNA) further demonstrated that Ex-4 preserved the tubular structure and suppressed mtDNA leakage into the cytosol (Fig. 5H−J). The levels of mitochondrial oxidative phosphorylation (OXPHOS), a cocktail of antibodies including five representative proteins of the electron transport complexes, were up-regulated by Ex-4 (Fig. 5K and L). Moreover, the Ex-4 treatment significantly preserved the cell viability under PA treatment (Fig. 5M). Hitherto, our results suggest that GLP-1 RAs treatment preserves the mitochondrial integrity and the redox balance under lipotoxicity.

3.6. *Suppression of STING signaling by GLP-1 RAs in the ECs of diabetic retinas*

To explore how mitochondrial function mediated the protective effects of GLP-1 RAs in ECs, we performed GSEA analysis and identified a significant reduction of "response to DNA damage stimulus" and slight augmentation in type I interferons-related pathways (Fig. 6A). As the STING pathway is activated by leaked mtDNA[43], together with the evidence that GLP-1 RA suppressed mtDNA leakage, we proposed that GLP-1 RAs might inhibit STING signaling to exert a protective effect on ECs under diabetic conditions. Consistent with our previous report that STING protein level was induced in diabetic retinas[23], particularly in retinal vessels, we showed here that GLP-1 RA treatment suppressed STING expression (Fig. 6B and C). To exclude the systemic impact of intraperitoneal injection of GLP-1 RAs, we further performed intravitreal injection of Ex-4 to the mouse retinas. Consistently, up-regulated expression of p-TBK1 was detected in the retinal vessels of *db*/*db* mice, while intravitreal injection of Ex-4 reduced the levels of p-TBK1 (Fig. 6D and E). Taken together, this data suggests that GLP-1 RA directly suppresses the activation of STING signaling in retinal vessels, independent of its function on reducing blood glucose.

The FVM is speculated to originate from the retina, and is composed of similar cell types[27]. However, the distribution of *STING* mRNA in the FVM remains unclear. Therefore, we re-analyzed a public scRNA-seq dataset of the FVM from proliferative DR patients (GSE165784)[27], and discovered that the *STING* mRNA was most abundantly expressed in ECs (Fig. 6F). To explore the potential role of enriched *STING* mRNA levels, we further divided the cells into $STING^{high}$ and $STING^{low}$ subgroups. Interestingly, $STING^{high}$ ECs expressed higher levels of vascular cell adhesion molecule 1 (*VCAM-1*) and interleukin 1 beta (*IL1B*) (Fig. 6G and H), indicating elevated inflammatory response in these cells. Re-analysis of the scRNA-seq data of oxygen-induced retinopathy (OIR) (GSE150703)[28] indicated that, the OIR retinas possessed more ECs with increased expression of *Sting* and inflammatory factors like C−X−C motif chemokine ligand 12 (*Cxcl12*), NF-κB inhibitor zeta (*Nfkbiz*) and inhibitor of NF-κB subunit beta (*Ikbkb*) (Supporting Information Fig. S3A−S3C). In addition, the OIR retinas had more ECs to express higher mRNA levels of *Sting* and tight junction component *Tjp1*, a gene that encodes zonula occludens-1 (ZO-1), as well as angiogenic factors *Vegfa* and angiopoietin 2 (*Angt2*) (Fig. 6I−K). Notably, higher levels of *Sting* and dipeptidyl peptidase 4 (*Dpp4*) an endogenous enzyme that cleaves GLP-1, were also detected in the ECs from the OIR retinas (Fig. S3D), indicating a potential crosstalk

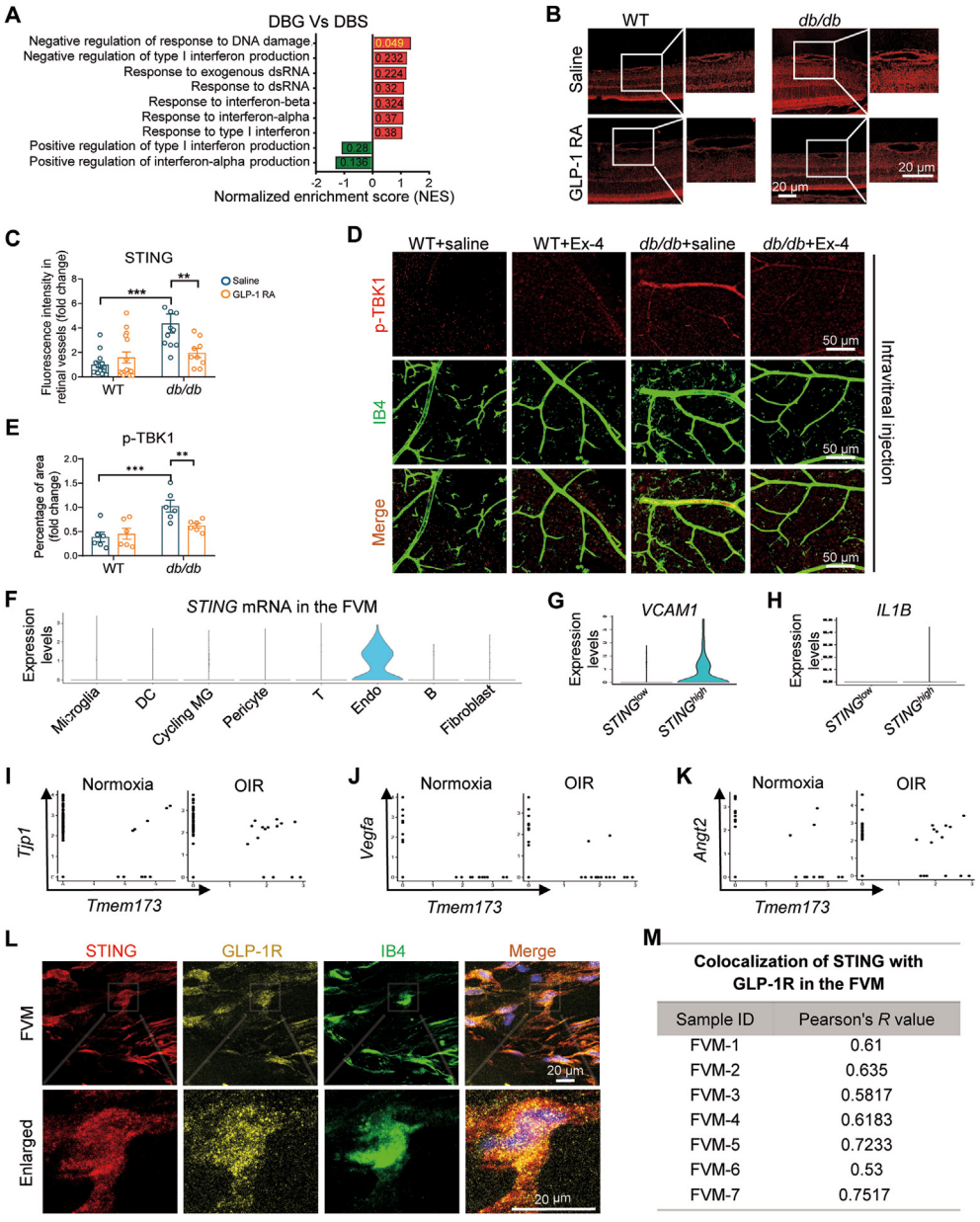

Sample ID	Pearson's *R* value
FVM-1	0.61
FVM-2	0.635
FVM-3	0.5817
FVM-4	0.6183
FVM-5	0.7233
FVM-6	0.53
FVM-7	0.7517

Figure 6 GLP-1 RAs suppressed the activation of STING signaling in the retinal vessels of DR. (A) GSEA of the STING-related pathways in the DBG retinas compared to the DBS controls. (B) Immunostaining and (C) quantification of STING (red) in the retinal sections of 18-week-old mice ($n = 5$, scale bar = 20 μm). (D) Immunostaining of p-TBK1 (red) and IB4 (green), and (E) quantification of p-TBK1 in the retinal flatmounts from mice receiving intravitreal injection of either saline or Ex-4 twice ($n = 3$ eyes, scale bar = 50 μm). (F) UMAP plot of cellular *STING* mRNA levels in the FVM from type 2 diabetic patients with proliferative DR. (G, H) Expression levels of *VCAM-1* and *IL-1B* mRNAs in the $STING^{high}$ and $STING^{low}$ ECs of the FVM from type 2 diabetic patients with proliferative DR. (I–K) Correlation of *Sting* mRNA expression with the levels of *Tjp1*, *Vegfa*, *Angt2*, and *Dpp4* in the ECs from the retinas of mice with/without OIR. (L) Immunostaining of STING (red), GLP-1R (yellow), IB4 (green), and (M) quantification of the colocalization percentage of GLP-1R with STING in the FVM from type 2 diabetic patients with proliferative DR ($n = 7$, scale bar = 20 μm). RNA-seq analyses and staining of STING together with GLP-1R were performed on the mice using loxenatide. Data are expressed as mean ± SEM; $^{*}P < 0.05$, $^{**}P < 0.01$, $^{***}P < 0.001$.

between GLP-1 and STING signaling pathways. Interestingly, GLP-1R and STING proteins were largely co-localized in the FVM, with a percentage ranging from 58% to 75% (Fig. 6L and M). In particular, GLP-1R and STING double-positive cells were predominantly IB4-positive, suggesting the exclusive distribution of GLP-1R and STING in either ECs or microglia. These data indicate that GLP-1 RAs suppress STING signaling in the vascular ECs of diabetic retinas.

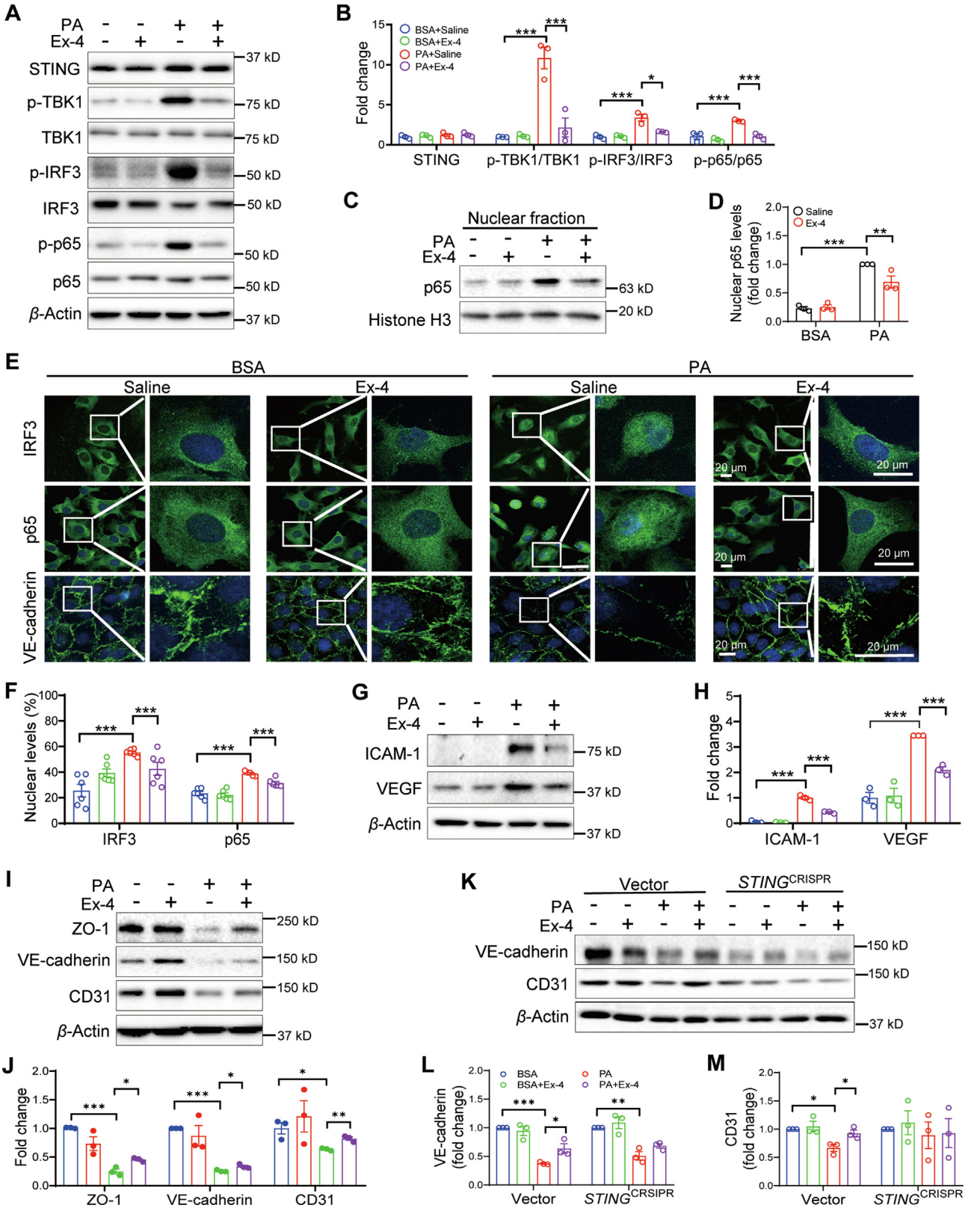

Figure 7 GLP-1 RA attenuated the activation of STING signaling to protect endothelial junction in HRVECs. (A–D, G–J) Western blot analysis and densitometry quantification of STING, p-TBK1, TBK1, p-p65, p65, p-IRF3, IRF3, ICAM-1, VEGF, ZO-1, VE-cadherin and CD31 in whole cell lysates, as well as p65 in the nuclear fractions in HRVECs pre-treated by Ex-4 (200 nmol/L) for 24 h, followed by treatment of PA (200 μmol/L) or BSA for 24 h ($n = 3$). (E, F) Immunostaining and quantification of p65, IRF3, and VE-cadherin in HRVECs pre-treated by Ex-4 (200 nmol/L) for 24 h, followed by treatment of PA (200 μmol/L) or BSA for 24 h ($n = 6$, scale bar = 20 μm). (K–M) Western blot analysis and densitometry quantification of VE-cadherin, CD31, and STING in the Vector and *STING*^{CRISPR} HRVECs pre-treated by Ex-4 (200 nmol/L) for 24 h, followed by treatment of PA (200 μmol/L) or BSA for 24 h ($n = 3$). Data are expressed as mean ± SEM; $^{*}P < 0.05$, $^{**}P < 0.01$, $^{***}P < 0.001$.

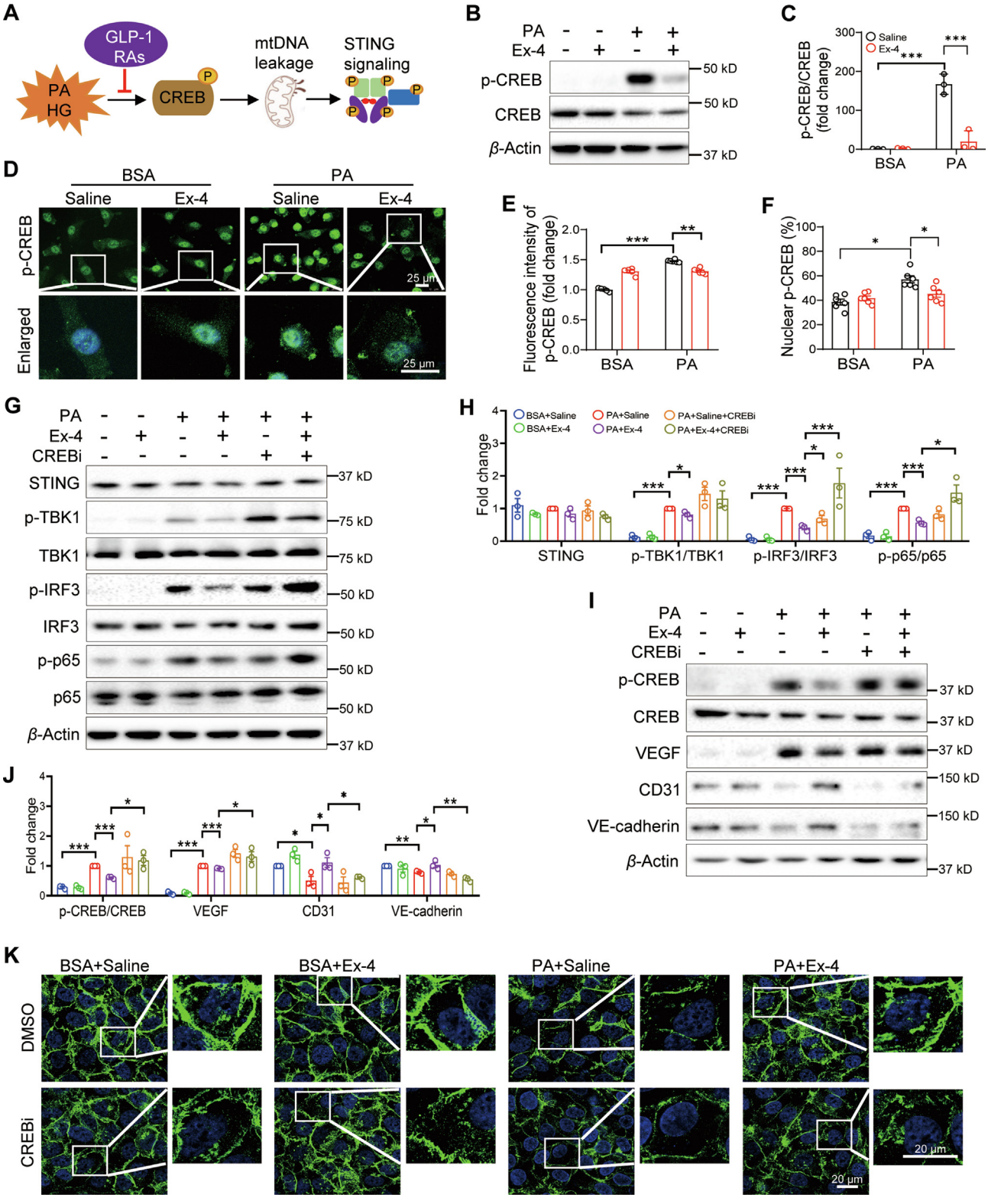

Figure 8 CREB was the downstream effector of GLP-1 RA in the regulation of STING signaling in retinal ECs. (A) Cartoon illustration of CREB as the downstream effector of GLP-1 RAs to inhibit mtDNA leakage into the cytosol in retinal vascular ECs. (B, C) Western blot analysis and densitometry quantification of p-CREB and CREB in HRVECs pre-treated by Ex-4 (200 nmol/L) for 24 h, followed by treatment of PA (200 μmol/L) or BSA for 24 h ($n = 3$). (D–F) Immunostaining of p-CREB and quantification of total p-CREB as well as nuclear p-CREB in HRVECs pre-treated by Ex-4 (200 nmol/L) for 24 h, followed by treatment of PA (200 μmol/L) or BSA for 24 h ($n = 6$, scale bar = 25 μm). (G–J) Western blot analysis and densitometry quantification of STING, p-TBK1, TBK1, p-p65, p65, p-IRF3, IRF3, p-CREB, CREB, VEGF, CD31, and VE-cadherin, and (K) staining of VE-cadherin in HRVECs pre-treated by Ex-4 (200 nmol/L) for 24 h and CREBi (100 nmol/L) for 2 h, followed by treatment of PA (200 μmol/L) or BSA for 24 h ($n = 3$, scale bar = 20 μm). Data are expressed as mean ± SEM; $^{*}P < 0.05$, $^{**}P < 0.01$, $^{***}P < 0.001$.

3.7. Attenuation of STING signaling and protection of endothelial junction in retinal ECs by GLP-1 RA treatment

To investigate whether GLP-1 RA could regulate STING signaling in retinal ECs under diabetic conditions, we co-treated HRVECs by Ex-4 together with PA or HG. As expected, PA and HG promoted the activation of STING signaling in HRVECs, as indicated by augmentation in p-TBK1/TBK1, p-NF-κB/NF-κB, and p-IRF3/IRF3, as well as increased nuclear levels of p65, while Ex-4 treatment reversed the above induction by PA and HG (Fig. 7A−F, Supporting Information Fig. S4A and S4B). In addition, Ex-4 treatment suppressed the levels of intercellular adhesion molecule 1 (ICAM-1) and VEGF, whereas up-regulated endothelial marker CD31 as well as junctional proteins ZO-1 and VE-cadherin (Fig. 7G−J). Immunostaining further showed that Ex-4 prohibited the nuclear translocation of p65 and IRF3, as well as VE-cadherin translocation away from the endothelial junction (Fig. 7E and F).

To further demonstrate whether STING signaling mediated the effects of GLP-1 RA, we generated *STING*^{CRISPR} HRVECs. Indeed, knockout of *STING* in HRVECs blunted the activation of STING signaling, as well as reversed the reduction of VE-cadherin and CD31 induced by PA; treatment of Ex-4 failed to reverse these changes in *STING*^{CRISPR} cells (Fig. 7K−M, Supporting Information Fig. S5E and S5F), indicating that STING signaling mediated the protective effect of GLP-1 RA. Notably, the protein levels of OXPHOS components were unaffected by *STING* knockout (Fig. S5G andS5 H), which confirmed our hypothesis that the functional changes of the mitochondria were upstream of STING signaling. In summary, these data demonstrate that GLP-1 RA prohibits STING signaling-elicited inflammation and breakdown of endothelial junctions.

3.8. Identification of CREB as the downstream effector of GLP-1 RA in the regulation of STING signaling in retinal ECs

As STING anchors on the endoplasmic reticulum membrane[44], there should be a mediator to transduce GLP-1 signaling to the STING pathway components. It is reported that CREB is a downstream effector of GLP-1 signaling in the regulation of glucose homeostasis[45], and also is an important mitochondrial regulator that controls differentiation, metabolism, and survival[46]. Therefore, we proposed that CREB might be the mediator of GLP-1 RA in regulating STING signaling (Fig. 8A). First, we examined the response of HRVECs to Ex-4. The data showed induction of p-CREB by Ex-4 treatment at 0.25 h (Supporting Information Fig. S6A and S6B). Interestingly, PA treatment for 24 h also significantly up-regulated the levels of p-CREB (Fig. S6D and S6E), while treatment of Ex-4 potently reduced the levels and nuclear translocation of p-CREB (Fig. 8B−F). To further demonstrate whether CREB was the downstream effector of GLP-1 RAs on regulating STING signaling, a chemical inhibitor for CREB (CREBi), 666-15 was utilized[25]. Indeed, Ex-4 suppressed the activation of STING signaling induced by PA; after treatment of CREBi, the inhibitory effect of Ex-4 on STING signaling was abolished, as indicated by increased levels of p-TBK1/TBK1 and p-IRF3/IRF3 (Fig. 8G and H). This effect was recapitulated in primary BMECs from WT mice (Supporting Information Fig. S7). We then tested the change on the endothelial junction after the application of CREBi. Accordingly, the restoration of VE-cadherin and ZO-1 by Ex-4 was prohibited by CREBi (Fig. 8I and J). Moreover, Ex-4-induced redistribution of VE-cadherin to the junctional area was also abrogated by CREBi (Fig. 8K). Taken together, we conclude that GLP-1 RA, at least partially, inhibits the STING pathway through the mediation of CREB to protect the integrity of endothelial junctions under diabetic conditions.

4. Discussion

GLP-1 deficiency is associated with diabetes and its complications[47]. However, GLP-1's functions in the retina, and its association with DR progression were unclear. Our study demonstrates that taking medication of GLP-1 RAs is associated with reduced DR incidences in a retrospective cohort study of type 2 diabetic patients. Our study also identified relatively high expression levels of GLP-1R in the retinal vasculature, which was downregulated under diabetic conditions. Further, we tested two different GLP-1 RAs in *db*/*db* mice, and confirmed the protective effect of GLP-1 RAs on retinal vessels under diabetic stress. Mechanistically, we demonstrated that STING signaling was the downstream cascade of GLP-1 RAs. To the best of our knowledge, this study is the first report to show that GLP-1 RA regulates the activation of STING, which provides a new insight into the crosstalk between GLP-1 signaling and STING signaling under diabetic conditions.

The debate on GLP-1 RAs' association with DR has intensified since the release of the SUSTAIN-6 study[7]. Later, a few meta-analyses[35,48] gave plausible explanations for this confliction: either because of insufficient follow-up duration to observe the overt progression of DR, which only averaged 3.4 years with huge variance between different studies, or because of incomplete baseline data collection for DR patients. Moreover, DPP-4 inhibitors, which potentiate GLP-1 signaling, were reported to be neutral on diabetic MVC[49]. In contrast, our retrospective cohort study revealed an improvement in DR-related symptoms by the treatment of GLP-1 RAs, with the median follow-up period being 2.8 years. HbA1c was demonstrated to be closely correlated with the progression of DR[35]. When additionally adjusting for HbA1c, the use of GLP-1 RAs remained significantly associated with the lower incidence of DR (Model 2). However, after justification by multiple confounder factors, no significant association was observed between GLP-1 Ras and the risk of DR (Model 3). Of note, our cohort has some limitations, such as, it is a retrospective cohort study instead of a randomized control trial, the limited sample size is enrolled in the GLP-1 RAs group, the follow-up period is shorter than 5 years which is suggested for observation of overt DR changes, and possible GLP-1 RAs users are unidentified in the insulin and OAD groups due to incomplete records. In addition, some important clinical characteristics such as the duration of diabetes, are missing, which may lead to incomplete adjustment for potential confounding factors. Therefore, a large-scale multicenter randomized clinical trial, with the primary outcome setting as DR-related symptoms, is recommended in the future to systemically and scrupulously evaluate the effect of GLP-1 RAs on DR progression.

Regardless of the debate in the clinical data, GLP-1 RAs have been proven in DR prevention, for instance, prevention of neurodegeneration[13], reduction of astrocyte transformation and retinal ganglion cell death[50], and prohibition of mononuclear phagocytes from infiltrating and secreting inflammatory cytokines[16]. Topical administration of GLP-1 RAs eye drops on *db*/*db* mice[13] and streptozotocin-induced diabetic rats[51] further confirmed the protective effect of GLP-1 RAs on retinopathy, which was

independent of its role in reducing blood glucose levels. However, few studies focused on the effect of GLP-1 RAs on the vascular integrity and functions related to DR. Actually, the effects of GLP-1 RAs on endothelial proliferation and tube formation were also controversial in different studies[9,52]. However, it is unquestionable that GLP-1 RAs protect vascular ECs from damage. Even though we did not exclude the possibility in this manuscript that the retina could partially benefit from reduced blood glucose through intraperitoneal administration of GLP-1 RAs, the two studies above, together with our intravitreal injection data in *db*/*db* mice and the results in retinal endothelial cells, demonstrated that GLP-1 RAs could directly protect the retina independent of reducing blood glucose.

The expression levels and distribution patterns of GLP-1R in the retina were also inconsistent[13,36]. A previous study reported a moderate expression of GLP-1R in the ganglion cell layer of human retinas[13]. However, according to the Uniprot database, GLP-1R was moderately expressed in arteries. Several studies also showed high expression of GLP-1R in ECs[53−55]. Consistently, enriched mRNA expression of GLP-1R was identified in the retinal vessels by scRNA-seq analysis and immunostaining in this study. To verify the specificity of the immunostaining, the specificity of the GLP-1R antibody, purchased from the Developmental Studies Hybridoma Bank (Catalogue No. Mab 7F38), was tested in HRVECs. After knocking down GLP-1R by adenovirus expressing shGLP-1R, a significant reduction of GLP-1R was detected (Supporting Information Fig. S8C), confirming the specificity of the GLP-1R antibody. Notably, long-term administration of GLP-1 RA significantly down-regulated the expression of GLP-1R in WT retinas, but restored the decreased levels of GLP-1R in diabetic retinas (Fig. S8A and S8B). Regarding the mRNA levels of GLP-1R, we also noticed the discrepant outcomes by different techniques, as GLP-1R was not detected in the databases of human FVM and mouse OIR retinas. However, according to our own sets of RNA-seq data from mouse retinas, *Glp1r* mRNA was moderately expressed. Moreover, we also referred to previous databases to search for *Glp1r* mRNA expression. In alignmol/Lent with our datasets, the expression of *Glp1r* mRNA was also detectable by microarray in the GSE10528 database. Therefore, the inconsistent results of GLP-1R mRNA expression levels may be attributed to different sequencing depths.

A recent report demonstrated that deletion of GLP-1R in brain astrocytes impaired the oxygen consumption rate and mitochondrial adaptation[41], suggesting the role of GLP-1 signaling in maintaining mitochondrial functions. Our study further strengthened the findings above as Ex-4 treatment preserved the mitochondrial integrity and maintained the redox balance in HRVECs. We further identified CREB in mediating the regulation of STING signaling by GLP-1 RAs. Notably, our study failed to detect the response of AKT signaling to Ex-4 stimulation (Fig. S6C), another downstream branch of GLP-1 RAs, suggesting CREB as the major effector of GLP-1 RAs in retinal ECs under diabetic conditions.

Enrichment of STING proteins was identified in the ECs from both OIR retinas and FVMs, which were more migratory and provocative, leading to the hypothesis that STING signaling may play important roles in inducing endothelial dysfunctions. Analysis of public scRNA-seq datasets revealed that STING activation was associated with endothelial inflammation and angiogenesis. Specific activation by a STING agonist, cGAMP, significantly up-regulated the levels of CD31, ZO-1, and VE-cadherin (Fig. S5C and S5D), whereas knockout of *STING* in HRVECs ameliorated the PA-induced reduction of these proteins (Fig. 7K, L, and Fig. S5E−S5H), which confirmed the pathogenic role of STING signaling in endothelial damage. However, the mechanistic roles of STING activation in endothelial migration and angiogenesis remain to be investigated. It is noteworthy that Ex-4 also inhibited cGAMP-induced activation of STING signaling (Fig. S5A and S5B), indicating a pathway independent of CREB to mediate the role of GLP-1 RAs' in regulating the STING signaling.

5. Conclusions

This study demonstrates the protective effects of GLP-1 RAs on DR pathogenesis at three levels: type 2 diabetic patients, type 2 diabetic mice, and retinal endothelial cells. It is the first report, to the best of our knowledge, that GLP-1 RAs protect endothelial junctions through inhibition of STING signaling. By investigating the underlying molecular mechanism, we reveal CREB as the mediator that transduces GLP-1 action to STING signaling in retinal ECs. Therefore, this study provides experimental evidence for the possibility of expanding GLP-1 RAs to the treatment of DR or diabetic vascular diseases.

Acknowledgments

We gratefully thank Dr. Jian-xing Ma (Wake Forest University, Winston-Salem, NC, USA) for his constructive suggestions and revision of this manuscript. This work was supported by grants from the National Natural Science Foundation of China (82000782, 82270886, 82070811), the Foster Program for NSFC at the Third Affiliated Hospital of Sun Yat-Sen University (2020G2RPYQN11, China), China International Medical Foundation (2018-N-01), and the Science and Technology Plan Project of Guangzhou City (2024A03J0002, China), Key Area R&D Program of Guangdong Province (2019B020227003, China), Sci-Tech Research Development Program of Guangzhou City (202201020589, China).

Author contributions

Yanming Chen designed the project, provided funding, and revised the manuscript. Xuemin He designed and performed experiments, and provided funding. Guojun Shi provided constructive suggestions and funding. Siying Wen, Xixiang Tang, Zheyao Wen, Rui Zhang, Shasha Li, Rong Gao, Jin Wang, Shiyi Wen, Ting Li, Li Zhou, and Heying Ai performed the experiments. Shaochong Zhang, Ruiping Peng, Dong Fang, and Zhaotian Zhang collected the human fibrovascular membranes. Yanhua Zhu and Yan Lu provided constructive suggestions.

Conflicts of interest

The authors declare no conflicts of interest.

Appendix A. Supporting information

Supporting data to this article can be found online at https://doi.org/10.1016/j.apsb.2024.03.011.

References

1. Teo ZL, Tham YC, Yu M, Chee ML, Rim TH, Cheung N, et al. Global prevalence of diabetic retinopathy and projection of burden through 2045: systematic review and meta-analysis. *Ophthalmology* 2021;**128**: 1580−91.

2. Wang L, Gao P, Zhang M, Huang Z, Zhang D, Deng Q, et al. Prevalence and ethnic pattern of diabetes and prediabetes in China in 2013. *JAMA* 2017;**317**:2515−23.
3. Kazemian P, Shebl FM, McCann N, Walensky RP, Wexler DJ. Evaluation of the cascade of diabetes care in the United States, 2005−2016. *JAMA Intern Med* 2019;**179**:1376−85.
4. Campbell JP, Zhang M, Hwang TS, Bailey ST, Wilson DJ, Jia Y, et al. Detailed vascular anatomy of the human retina by projection-resolved optical coherence tomography angiography. *Sci Rep* 2017;**7**:42201.
5. Schmidt M, Giessl A, Laufs T, Hankeln T, Wolfrum U, Burmester T. How does the eye breathe? Evidence for neuroglobin-mediated oxygen supply in the mammalian retina. *J Biol Chem* 2003;**278**:1932−5.
6. Duh EJ, Sun JK, Stitt AW. Diabetic retinopathy: current understanding, mechanisms, and treatment strategies. *JCI Insight* 2017;**2**:e93751.
7. Marso SP, Bain SC, Consoli A, Eliaschewitz FG, Jodar E, Leiter LA, et al. Semaglutide and cardiovascular outcomes in patients with type 2 diabetes. *N Engl J Med* 2016;**375**:1834−44.
8. Marso SP, Daniels GH, Brown-Frandsen K, Kristensen P, Mann JF, Nauck MA, et al. Liraglutide and cardiovascular outcomes in type 2 diabetes. *N Engl J Med* 2016;**375**:311−22.
9. Gaborit B, Julla JB, Besbes S, Proust M, Vincentelli C, Alos B, et al. Glucagon-like peptide 1 receptor agonists, diabetic retinopathy and angiogenesis: the AngioSafe type 2 diabetes study. *J Clin Endocrinol Metab* 2020;**105**:dgz069.
10. Gerstein HC, Colhoun HM, Dagenais GR, Diaz R, Lakshmanan M, Pais P, et al. Dulaglutide and cardiovascular outcomes in type 2 diabetes (REWIND): a double-blind, randomised placebo-controlled trial. *Lancet* 2019;**394**:121−30.
11. Wang T, Lu W, Tang H, Buse JB, Sturmer T, Gower EW. Assessing the association between GLP-1 receptor agonist use and diabetic retinopathy through the FDA adverse event reporting system. *Diabetes Care* 2019;**42**:e21−3.
12. Chung YW, Lee JH, Lee JY, Ju HH, Lee YJ, Jee DH, et al. The anti-inflammatory effects of glucagon-like peptide receptor agonist lixisenatide on the retinal nuclear and nerve fiber layers in an animal model of early type 2 diabetes. *Am J Pathol* 2020;**190**:1080−94.
13. Hernandez C, Bogdanov P, Corraliza L, Garcia-Ramirez M, Sola-Adell C, Arranz JA, et al. Topical administration of GLP-1 receptor agonists prevents retinal neurodegeneration in experimental diabetes. *Diabetes* 2016;**65**:172−87.
14. Ding L, Zhang J. Glucagon-like peptide-1 activates endothelial nitric oxide synthase in human umbilical vein endothelial cells. *Acta Pharmacol Sin* 2012;**33**:75−81.
15. Sjoberg KA, Holst JJ, Rattigan S, Richter EA, Kiens B. GLP-1 increases microvascular recruitment but not glucose uptake in human and rat skeletal muscle. *Am J Physiol Endocrinol Metab* 2014;**306**:E355−62.
16. Zhou L, Xu Z, Oh Y, Gamuyao R, Lee G, Xie Y, et al. Myeloid cell modulation by a GLP-1 receptor agonist regulates retinal angiogenesis in ischemic retinopathy. *JCI Insight* 2021;**6**:e93382.
17. Helmstadter J, Frenis K, Filippou K, Grill A, Dib M, Kalinovic S, et al. Endothelial GLP-1 (glucagon-like peptide-1) receptor mediates cardiovascular protection by liraglutide in mice with experimental arterial hypertension. *Arterioscler Thromb Vasc Biol* 2020;**40**:145−58.
18. Bendotti G, Montefusco L, Lunati ME, Usuelli V, Pastore I, Lazzaroni E, et al. The anti-inflammatory and immunological properties of GLP-1 receptor agonists. *Pharmacol Res* 2022;**182**:106320.
19. Decout A, Katz JD, Venkatraman S, Ablasser A. The cGAS−STING pathway as a therapeutic target in inflammatory diseases. *Nat Rev Immunol* 2021;**21**:548−69.
20. Liu Y, Jesus AA, Marrero B, Yang D, Ramsey SE, Sanchez GAM, et al. Activated STING in a vascular and pulmonary syndrome. *N Engl J Med* 2014;**371**:507−18.
21. Mao Y, Luo W, Zhang L, Wu W, Yuan L, Xu H, et al. STING−IRF3 triggers endothelial inflammation in response to free fatty acid-induced mitochondrial damage in diet-induced obesity. *Arterioscler Thromb Vasc Biol* 2017;**37**:920−9.
22. Oduro PK, Zheng X, Wei J, Yang Y, Wang Y, Zhang H, et al. The cGAS−STING signaling in cardiovascular and metabolic diseases: future novel target option for pharmacotherapy. *Acta Pharm Sin B* 2022;**12**:50−75.
23. Wen Z, He X, Wang J, Wang H, Li T, Wen S, et al. Hyperlipidemia induces proinflammatory responses by activating STING pathway through IRE1α−XBP1 in retinal endothelial cells. *J Nutr Biochem* 2023;**112**:109213.
24. Liu H, Ghosh S, Vaidya T, Bammidi S, Huang C, Shang P, et al. Activated cGAS/STING signaling elicits endothelial cell senescence in early diabetic retinopathy. *JCI Insight* 2023;**8**:e168945.
25. Xie F, Li BX, Kassenbrock A, Xue C, Wang X, Qian DZ, et al. Identification of a potent inhibitor of CREB-mediated gene transcription with efficacious *in vivo* anticancer activity. *J Med Chem* 2015;**58**:5075−87.
26. Tabula Sapiens C, Jones RC, Karkanias J, Krasnow MA, Pisco AO, Quake SR, et al. The Tabula sapiens: a multiple-organ, single-cell transcriptomic atlas of humans. *Science* 2022;**376**:eabl4896.
27. Hu Z, Mao X, Chen M, Wu X, Zhu T, Liu Y, et al. Single-cell transcriptomics reveals novel role of microglia in fibrovascular membrane of proliferative diabetic retinopathy. *Diabetes* 2022;**71**:762−73.
28. Crespo-Garcia S, Tsuruda PR, Dejda A, Ryan RD, Fournier F, Chaney SY, et al. Pathological angiogenesis in retinopathy engages cellular senescence and is amenable to therapeutic elimination *via* BCL-xL inhibition. *Cell Metabol* 2021;**33**:818−32.e7.
29. Qiu F, Matlock G, Chen Q, Zhou K, Du Y, Wang X, et al. Therapeutic effects of PPARα agonist on ocular neovascularization in models recapitulating neovascular age-related macular degeneration. *Invest Ophthalmol Vis Sci* 2017;**58**:5065−75.
30. Lee H, Lee M, Chung H, Kim HC. Quantification of retinal vessel tortuosity in diabetic retinopathy using optical coherence tomography angiography. *Retina* 2018;**38**:976−85.
31. Wu W, Takahashi Y, Shin HY, Ma X, Moiseyev G, Ma JX. The interplay of environmental luminance and genetics in the retinal dystrophy induced by the dominant RPE65 mutation. *Proc Natl Acad Sci U S A* 2022;**119**:e2115202119.
32. Ruck T, Bittner S, Epping L, Herrmann AM, Meuth SG. Isolation of primary murine brain microvascular endothelial cells. *J Vis Exp* 2014;(93):e52204.
33. Zudaire E, Gambardella L, Kurcz C, Vermeren S. A computational tool for quantitative analysis of vascular networks. *PLoS One* 2011;**6**:e27385.
34. Tang X, Tan Y, Yang Y, Li M, He X, Lu Y, et al. Association of the monocyte-to-high-density lipoprotein cholesterol ratio with diabetic retinopathy. *Front Cardiovasc Med* 2021;**8**:707008.
35. Bethel MA, Diaz R, Castellana N, Bhattacharya I, Gerstein HC, Lakshmanan MC. HbA1c change and diabetic retinopathy during GLP-1 receptor agonist cardiovascular outcome trials: a meta-analysis and meta-regression. *Diabetes Care* 2021;**44**:290−6.
36. Hebsgaard JB, Pyke C, Yildirim E, Knudsen LB, Heegaard S, Kvist PH. Glucagon-like peptide-1 receptor expression in the human eye. *Diabetes Obes Metabol* 2018;**20**:2304−8.
37. Bogdanov P, Corraliza L, Villena JA, Carvalho AR, Garcia-Arumi J, Ramos D, et al. The *db/db* mouse: a useful model for the study of diabetic retinal neurodegeneration. *PLoS One* 2014;**9**:e97302.
38. Sasongko MB, Wong TY, Nguyen TT, Cheung CY, Shaw JE, Wang JJ. Retinal vascular tortuosity in persons with diabetes and diabetic retinopathy. *Diabetologia* 2011;**54**:2409−16.
39. Luo Y, Xiao W, Zhu X, Mao Y, Liu X, Chen X, et al. Differential expression of claudins in retinas during normal development and the angiogenesis of oxygen-induced retinopathy. *Invest Ophthalmol Vis Sci* 2011;**52**:7556−64.
40. Arima M, Nakao S, Yamaguchi M, Feng H, Fujii Y, Shibata K, et al. Claudin-5 redistribution induced by inflammation leads to anti-VEGF-resistant diabetic macular edema. *Diabetes* 2020;**69**:981−99.
41. Timper K, Del Rio-Martin A, Cremer AL, Bremser S, Alber J, Giavalisco P, et al. GLP-1 receptor signaling in astrocytes regulates fatty acid oxidation, mitochondrial integrity, and function. *Cell Metabol* 2020;**31**:1189−205.e13.

42. Perelman A, Wachtel C, Cohen M, Haupt S, Shapiro H, Tzur A. JC-1: alternative excitation wavelengths facilitate mitochondrial membrane potential cytometry. *Cell Death Dis* 2012;**42**:17−28.
43. Yu CH, Davidson S, Harapas CR, Hilton JB, Mlodzianoski MJ, Laohamonthonkul P, et al. TDP-43 triggers mitochondrial DNA release *via* mPTP to activate cGAS/STING in ALS. *Cell* 2020;**183**: 636−49.e18.
44. Lu D, Shang G, Li J, Lu Y, Bai XC, Zhang X. Activation of STING by targeting a pocket in the transmembrane domain. *Nature* 2022;**604**: 557−62.
45. Lee JH, Wen X, Cho H, Koo SH. CREB/CRTC2 controls GLP-1-dependent regulation of glucose homeostasis. *FASEB J* 2018;**32**: 1566−78.
46. Geary K, Knaub LA, Schauer IE, Keller AC, Watson PA, Miller MW, et al. Targeting mitochondria to restore failed adaptation to exercise in diabetes. *Biochem Soc Trans* 2014;**42**:231−8.
47. Gribble FM, Reimann F. Metabolic messengers: glucagon-like peptide 1. *Nat Metab* 2021;**3**:142−8.
48. Wang F, Mao Y, Wang H, Liu Y, Huang P. Semaglutide and diabetic retinopathy risk in patients with type 2 diabetes mellitus: a meta-analysis of randomized controlled trials. *Clin Drug Invest* 2022;**42**: 17−28.
49. Taylor OM, Lam C. The effect of dipeptidyl peptidase-4 inhibitors on macrovascular and microvascular complications of diabetes mellitus: a systematic review. *Curr Ther Res Clin Exp* 2020;**93**:100596.
50. Sterling JK, Adetunji MO, Guttha S, Bargoud AR, Uyhazi KE, Ross AG, et al. GLP-1 receptor agonist NLY01 reduces retinal inflammation and neuron death secondary to ocular hypertension. *Cell Rep* 2020;**33**:108271.
51. Wang YC, Wang L, Shao YQ, Weng SJ, Yang XL, Zhong YM. Exendin-4 promotes retinal ganglion cell survival and function by inhibiting calcium channels in experimental diabetes. *iScience* 2023;**26**:107680.
52. Aronis KN, Chamberland JP, Mantzoros CS. GLP-1 promotes angiogenesis in human endothelial cells in a dose-dependent manner, through the Akt, Src and PKC pathways. *Metabolism* 2013;**62**: 1279−86.
53. Nystrom T, Gutniak MK, Zhang Q, Zhang F, Holst JJ, Ahren B, et al. Effects of glucagon-like peptide-1 on endothelial function in type 2 diabetes patients with stable coronary artery disease. *Am J Physiol Endocrinol Metab* 2004;**287**:E1209−15.
54. Ishibashi Y, Matsui T, Takeuchi M, Yamagishi S. Glucagon-like peptide-1 (GLP-1) inhibits advanced glycation end product (AGE)-induced up-regulation of VCAM-1 mRNA levels in endothelial cells by suppressing AGE receptor (RAGE) expression. *Biochem Biophys Res Commun* 2010;**391**:1405−8.
55. Ban K, Noyan-Ashraf MH, Hoefer J, Bolz SS, Drucker DJ, Husain M. Cardioprotective and vasodilatory actions of glucagon-like peptide 1 receptor are mediated through both glucagon-like peptide 1 receptor-dependent and -independent pathways. *Circulation* 2008;**117**: 2340−50.